Clim Dyn (2017) 48:3459–3474
DOI 10.1007/s00382-016-3278-1

Strong effects of tropical ice-sheet coverage and thickness on the hard snowball Earth bifurcation point

Yonggang Liu[1] · W. Richard Peltier[2] · Jun Yang[1] · Guido Vettoretti[2] · Yuwei Wang[1]

Received: 29 July 2015 / Accepted: 15 July 2016 / Published online: 19 July 2016

Abstract The hard snowball Earth bifurcation point is determined by the level of atmospheric carbon dioxide concentration (pCO_2) below which complete glaciation of the planet would occur. In previous studies, the bifurcation point was determined based on the assumption that the extent of continental glaciation could be neglected and the results thereby obtained suggested that very low values of pCO_2 would be required (~100 ppmv). Here, we deduce the upper bound on the bifurcation point using the coupled atmosphere–ocean climate model of the NCAR that is referred to as the Community Climate System Model version 3 by assuming that the continents are fully covered by ice sheets prior to executing the transition into the hard snowball state. The thickness of the ice sheet is assumed to be that obtained by an ice-sheet model coupled to an energy balance model for a soft snowball Earth. We find that the hard snowball Earth bifurcation point is in the ranges of 600–630 and 300–320 ppmv for the 720 and 570 Ma continental configurations, respectively. These critical points are between 10 and 3 times higher than their respective values when ice sheets are completely neglected. We also find that when the ice sheets are thinner than those assumed above, the climate is colder and the bifurcation point is larger. The key process that causes the excess cooling when continental ice sheets are thin is shown to be associated with the fact that atmospheric heat transport from the adjacent oceans to the ice sheet-covered continents is enhanced in such conditions. Feedbacks from sea-ice expansion and reduced water vapor concentration further cool the oceanic regions strongly.

Keywords Snowball Earth · Bifurcation point · Tropical ice sheet · Atmospheric heat transport · Neoproterozoic

1 Introduction

Several global glaciations are inferred to have occurred during the Neoproterozoic Era of Earth history (1000–540 Ma) (Ma = million years ago; e.g., Hoffman et al. 1998; Hoffman and Schrag 2000, 2002), in which the continents are suggested to have been completely covered by thick ice sheets with perhaps only isolated islands remaining ice free (e.g., Hyde et al. 2000) and the oceans largely covered by sea ice. The extent of sea-ice cover during these glaciation events remains unconstrained, due to the complete removal of relevant sedimentary records by the subduction of ocean floor. The terms of "hard snowball" or "soft snowball/slushball" have been applied to the states in which sea ice either fully or only partially covered the oceans, respectively. Regardless of which of these states best characterized the Neoproterozoic glacial climate, it must have been extremely cold. It is important, however, to know the magnitude of climate forcing, which is required for the Earth to enter either of these snowball Earth states as this may help identify the mechanisms that gave rise to the occurrence of these states.

The weaker solar luminosity of the Neoproterozoic Era (Gough 1981; Bahcall et al. 2001) was one important condition that enabled deep glaciation to occur but one that by itself would have been insufficient for the formation of either hard or soft snowball climate states; previous

✉ Yonggang Liu
ygliu@pku.edu.cn

[1] Department of Atmospheric and Oceanic Sciences, School of Physics, Peking University, Beijing 100871, China

[2] Department of Physics, University of Toronto, 60 St. George Street, Toronto, ON M5S 1A7, Canada

Table 1 An incomplete list of studies (many other studies especially the early EBM studies determine the snowball bifurcation point in terms of the reduction of solar constant, not pCO_2) that have determined the snowball bifurcation points

Investigators	Model name	Model type	Continental configuration	Snowball bifurcation point (ppmv)[a]
Crowley et al. (2001), Peltier et al. (2007) and Liu and Peltier (2010)	EBM&UofT GSM	EBM but with active ice sheets	720 and 570 Ma	~100
Jenkins and Smith (1999)	GENESIS	AGCM	Idealized	~1700
Chandler and Sohl (2000)	GISS GCM	AGCM	~600 Ma	<40
Poulsen et al. (2002)	FOAM1.4	AOGCM	Idealized and 545 Ma	<140
Donnadieu et al. (2004)	CLIMBER-2	EMIC[b]	~800 Ma and present	~100
Lewis et al. (2007)	UNic ESCM	OGCM	Idealized	~4000
Voigt and Marotzke (2010)	ECHAM5/MPI-OM	AOGCM	Present-day	Not applicable
Voigt et al. (2011)	ECHAM5/MPI-OM	AOGCM	635 Ma	~500
Yang et al. (2012a)	CCSM3	AOGCM	Present-day	~20
Yang et al. (2012c)	CCSM4	AOGCM	Present-day	~70
Liu et al. (2013)	CCSM3	AOGCM	720 and 570 Ma	~100
This study	CCSM3	AOGCM	720 and 570 Ma with ice sheets	~600 (720 Ma) ~300 (570 Ma)

[a] The solar insolation is fixed to 94 % of present-day value in all studies except that in Poulsen et al. (2002) who use a solar insolation 93 % of present-day value

[b] EMIC stands for Earth system Models of Intermediate Complexity. Specifically for the CLIMBER-2 here, neither the atmosphere nor the ocean component is a GCM, but is more complex than EBM and mixed-layer ocean, respectively

analyses have demonstrated that the concentration of greenhouse gases would also have had to be sufficiently low. The solar luminosity would have evolved from one snowball Earth event to the next due to both the (crudely determined) duration of each event (4–30 million years; e.g., Hoffman et al. 1998; Bodiselitsch et al. 2005; Macdonald et al. 2010) and the significant period of time that separated the events. For example, the Sturtian glaciation occurred approximately 715 million years ago (Ma), while the Marinoan glaciation most probably occurred at approximately 650 Ma (Hoffman and Li 2009). The corresponding difference in solar insolation between the two periods is ~0.7 %, i.e., about 2.4 W m^{-2} in global mean. Although small, some researchers (e.g., Feulner and Kienert 2014) stressed that different solar insolation should be assumed to have been associated with each event. However, to simplify the comparison between different modeling studies, it has been considered more convenient to fix the solar luminosity to a certain value, say, 94 % of the present-day value. On this basis, we may then summarize the critical pCO_2 below which a hard snowball Earth would be expected to form (hereafter we refer to this critical pCO_2 for hard snowball Earth initiation as the "snowball bifurcation point") obtained in different studies and determine the most likely range of this snowball bifurcation point.

Recently, state-of-the-art coupled Atmosphere and Ocean General Circulation Models (AOGCMs) such as ECHAM5/MPI-OM (Voigt and Marotzke 2010; Voigt et al. 2011; Voigt and Abbot 2012) and Community Climate System Model version 3 (CCSM3) (Yang et al. 2012a, b; Liu et al. 2013) or CCSM4 (Yang et al. 2012c) have been used to determine the bifurcation point. When the (likely more realistic) value of sea-ice albedo employed in CCSM3 was also employed in ECHAM5/MPI-OM (Voigt and Abbot 2012), the bifurcation point was constrained by both models to the range of ~100–200 ppmv when solar insolation was reduced to 94 % of the present-day value. This smaller range of uncertainty is a significant improvement compared to the results obtained using atmosphere-only general circulation models (AGCMs). The range of pCO_2 determined using these AGCMs has been found to be as low as <40 ppmv (e.g., Chandler and Sohl 2000) or as high as ~1700 ppmv (e.g., Jenkins and Smith 1999). The latest results, especially those obtained using the CCSM model versions (~100 ppmv), are also consistent with those of the earlier work of Poulsen et al. (2001; 2002) and Poulsen and Jacob (Poulsen and Jacob 2004), who first employed an AOGCM [the FOAM model (Poulsen et al. 2001)] to argue that a hard snowball Earth could not form at a value of pCO_2 as low as 140 ppmv even when the solar insolation is 93 % of the present-day value (see Table 1 for a summary).

Previous AOGCM studies, however, have all neglected the influence of continental ice cover on the snowball bifurcation point. This is understandable since continental ice sheets evolve on a timescale of thousands of years or longer (for example the characteristic timescale of the Late Quaternary ice-age cycle that was significantly forced by orbital insolation variations was 100 thousand years (kyr)

(Shackleton et al. 1990); see also Liu and Peltier (2010) for an illustration of a similar timescale governing the occurrence of global glaciation). Although modern coupled AOGCMs may be run successfully on timescales of a few thousands of years, the resources required for longer integrations can be prohibitively expensive. As the first step towards understanding the influence of continental ice cover on the snowball bifurcation point, we will employ an initial condition in which the continents are assumed to be fully covered by ice but the tropical oceans to be free of sea ice so that the system is in a soft snowball climate state.

The results for the snowball bifurcation point that such analyses deliver will clearly be upper bounds on the CO_2 concentration at the bifurcation point; the surface albedo of the Earth is maximized by assuming a complete coverage of the low-albedo bare land by high-albedo ice. A hard snowball could form when the continents were only partially covered by ice, in which case the bifurcation point would certainly be lower due to smaller overall surface albedo. In reality, the continental ice sheets would first nucleate on relatively high latitude regions or high elevations (e.g., Rodehacke et al. 2013) of the supercontinent, they may thereafter flow to lower latitude or altitude. This is a very slow process; even if the concentration of greenhouse gases is appropriate, it takes many tens or even hundreds of thousands of years for the ice sheet to grow to cover the whole continent (Liu and Peltier 2010). If the concentration of greenhouse gases decreases very rapidly compared to this time scale of ice sheet growth, a hard snowball Earth may form when the coverage of the ice sheet is still sub-continental in scale because the growth of global sea ice takes only a few 100 years (e.g., Voigt and Marotzke 2010). In previous AOGCM studies, the formation of a hard snowball Earth (in terms of sea-ice coverage) was investigated in the absence of the existence of any continental ice sheets. These studies therefore implicitly assumed that the concentration of greenhouse gases decreased so rapidly that no ice sheets could form on the continents before the Earth entered a hard snowball state. In the present work, we assume that the concentration of greenhouse gases decreases slowly enough so that the continental ice sheets have sufficient time to respond and grow to their maximum possible extent.

The upper bounds on the snowball bifurcation point will be obtained herein for two different continental configurations subject to the above described initial condition, i.e. that the continental ice sheets have fully developed. Compared with previous analyses in which the influence of continental ice cover was neglected, the bifurcation point so determined will demonstrate how much more easily the hard snowball Earth may form. These upper bound results will also provide useful guidance for future more elaborate analyses in which transient ice sheet evolution into a state of Neoproterozoic glaciation is fully simulated using an ice-sheet model appropriately coupled to an AOGCM; an initial pCO_2 may be chosen for such transient analyses based on the results to be obtained herein. Testing whether a soft snowball Earth can or cannot form with such future analyses will be critical, as they will be much more credible than the analyses performed with an ice-sheet model coupled to an energy balance model (EBM) (e.g., Hyde et al. 2000; Liu and Peltier 2010).

As will be described in what follows, by using the AOGCM CCSM3 we do, unsurprisingly, find that the bifurcation point is much higher than that obtained under the assumption that no land ice is present on the continents. Moreover, we will demonstrate that thinner ice sheets produce colder climate under the same solar insolation and greenhouse gas concentrations, thus representing states that are more prone to transitioning into a hard snowball state than would be the case if the continental ice sheets were thick. This is contrary to what we had initially expected since lower surface elevation has higher surface temperature according to some adiabatic or moist adiabatic lapse rate based analyses. Given this unexpected result we will also carry out detailed analysis to identify the mechanism that supports the occurrence of colder climate when the continental ice sheets are thinner. For these additional analyses, as stated previously, we will employ the atmospheric component of CCSM3, i.e. the Community Atmosphere Model version 3 (CAM3). A detailed description of the numerical experiments we have performed is provided in Sect. 2. Results are described in Sect. 3, and conclusions are given in Sect. 4.

2 Design of a suite of Neoproterozoic climate simulations

2.1 Continental configurations

The two super-continental configurations employed herein are those for 720 and 570 Ma, previously employed by Liu and Peltier (2010, 2011) and Liu et al. (2013) and are distinguished from one another by their latitudinal positions (see Fig. 1). They were originally reconstructed by Li et al. (2008) and Dalziel (1997), respectively. We employ the 570 Ma configuration of Dalziel (1997) rather than the, perhaps more accurate Marinoan configuration of Li et al. (2008), in order to investigate the impact upon the results of a slightly less equatorially centered reconstruction of supercontinent position. This is potentially important because the accuracy of the paleomagnetic data on the basis of which such reconstructions are produced continues to be debated. For these analyses, the supercontinents are assumed to be flat (with 400 m freeboard) prior to emplacement of the ice

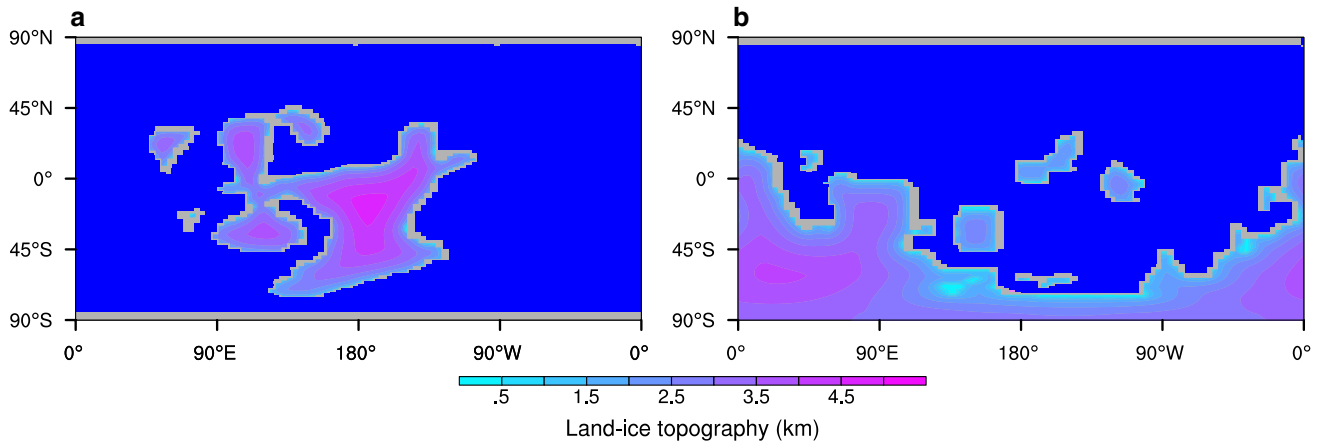

Fig. 1 Continental configurations (*grey*), almost completely covered by ice sheets whose surface elevation is shown in *blue-pink*. **a**, **b** For 720 and 570 Ma, respectively. The ocean is shown in *dark blue*. The ice extent does not perfectly match the continents because the ice-sheet model has different horizontal resolution from the CCSM3 climate model

sheets. Following the emplacement, the deformation of the bedrock surface and the fall of sea level associated with the extraction of water from the ocean basins required to build them are taken into account following the recent discussion of sea-level change during snowball Earth events by Liu and Peltier (2013a, b).

2.2 Ice-sheet configurations

The ice-sheet distributions are fixed to those previously determined for soft snowball Earth states by Liu and Peltier (2010) using a 3-D thermomechanical ice-sheet model based upon the shallow ice approximation coupled with an EBM (Fig. 1). It is important to note that the results obtained in this work and the conclusions that follow from them should not be impacted significantly by the choice of ice-sheet distribution so long as the ice sheets cover all the continents. The particular choice on which the current work is based has been solely on the basis of ease of implementation. The ice-sheet thicknesses delivered by other models may differ slightly, and we test the influence of this uncertainty on the determination of bifurcation point by testing the sensitivity of the result to reductions in ice-sheet thickness by varying amounts. The reasons why we are testing sensitivity to reductions in ice sheet thickness rather than increases are discussed below.

The elevations of the ice-sheet surface obtained in Liu and Peltier (2010) are similar to, but most probably slightly higher than those obtained by Donnadieu et al. (2003; see their Fig. 5d) using an ice-sheet model forced by climate fields from an AGCM. The elevations we employ are likely upper bounds because the parameterization in the EBM tends to overestimate the precipitation in the interior of the continents compared to that in general circulation models (GCMs) such as CCSM3. The EBM also completely ignores evaporation. Moreover, the EBM seems to underestimate the surface temperature in the tropical region compared to CCSM3, at least for a soft snowball Earth state (Fig. 2a, d). High surface temperature both increases surface melting and enhances ice dynamics. For these reasons, the surface mass balance is overestimated almost everywhere by the EBM (Fig. 2b) compared to the CCSM3 model (Fig. 2e). The thicknesses of the continental ice sheets calculated using the University of Toronto (UofT) Glacial System Model (GSM) (see Tarasov and Peltier 1999) for the two surface temperatures and surface mass balances are shown in Fig. 2c, f. This is one demonstration of the possible uncertainties in land-ice thickness due to the difference between ice-sheet models forced by the EBM and by a specific GCM; predictions based on the use of GCMs other than the CCSM3 may of course differ. Therefore, to test how the bifurcation point might be influenced by the uncertainties in the ice-sheet thickness, three more cases are analyzed in which the ice-sheet thickness is reduced uniformly to 75, 50 and 25 % of the original values used in Liu and Peltier (2010), respectively. These sensitivity analyses are performed only for the 720 Ma (Sturtian) continental configuration and associated ice sheets, since its more equatorially distributed supercontinent provides a more stringent test of the soft snowball Earth hypothesis; the formation of a soft snowball Earth on such continental configuration is more difficult than that on a supercontinent located more towards the poles (Liu and Peltier 2010). Further research on this topic involving coupled climate-ice-sheet modeling, to be discussed elsewhere, will be based on this Sturtian continental configuration.

The results we will obtain for the 50 and 25 % ice-sheet thickness cases will be interesting only from the perspective

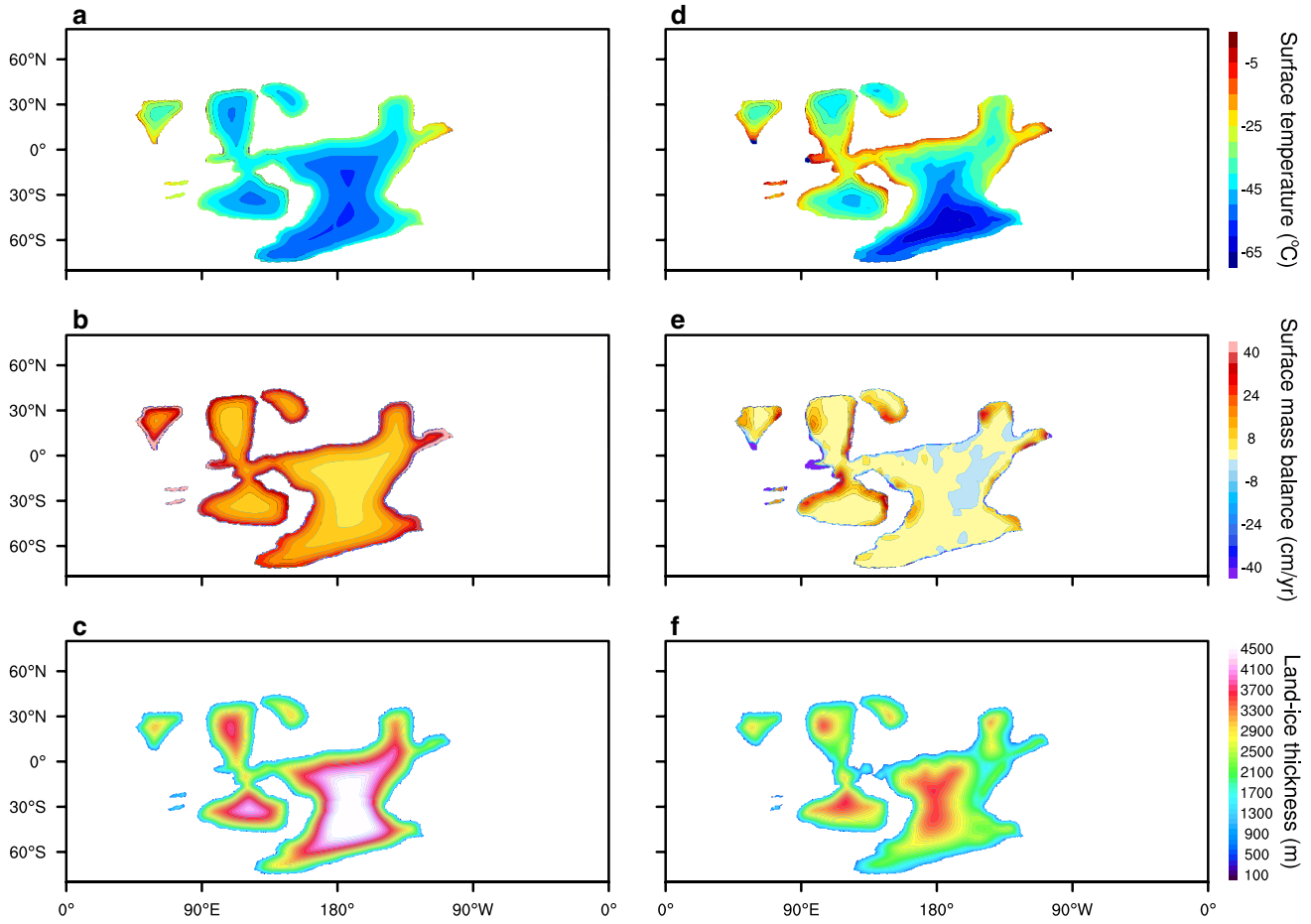

Fig. 2 **a**, **d** Surface temperature; **b**, **e** Surface mass balance (snow accumulation plus refreezing minus melting minus evaporation at the surface); **c**, **f** The ice thickness in equilibrium with the respective surface temperature (**a**, **d**) and surface mass balance (**b**, **e**). The panels on the *left* are from the energy balance model (EBM), and the ones on the *right* are from the CCSM3 climate model

of a sensitivity study as these are unlikely to be representative of Neoproterozoic conditions. This is because that the 100 % thickness case calculated by the UofT GSM coupled with an EBM is consistent with geological inference (Liu and Peltier 2013a, b); if the ice sheets are 50 % or more thinner than this control case, the sea level drop associated with their construction would be too small compared with observations (Hoffman et al. 2007). Further support for this argument is provided by the fact that the 100 % ice-sheet thickness adopted here is in fact close to that previously obtained by Donnadieu et al. (2003), in which the ice sheets were calculated for a hard snowball Earth state whose atmosphere should be much drier than the soft snowball Earth state (Yang et al. 2012a, b) assumed here.

2.3 CCSM3 configuration

As previously discussed we will be employing the CCSM3 model (Collins et al. 2006) to determine the bifurcation point. This model simulates four major components of the climate system, namely, atmosphere, ocean, land surface processes, and sea ice. The respective model components are the CAM3 atmospheric component, the Parallel Ocean Program (POP, based on version 1.4.3), the Community Land Model version 3 (CLM3), and the Community Sea Ice Model version 5 (CSIM5). These four components are linked through a flux coupler (CPL6), with no flux corrections between any two components. Both CAM3 and POP are 3-D general circulation models. CLM3 considers dynamic vegetation and explicit river routing although the river routing scheme plays no role in the analysis to be performed here. CSIM5 accounts for both thermodynamic and dynamic contributions to the thickness and distribution of sea ice.

The atmospheric concentrations of CH_4 (pCH_4) and N_2O (pN_2O) are assumed to be 805.6 and 276.7 ppbv, respectively, for the purpose of the analyses to be discussed herein. Aerosols are assumed to be spatially uniform and temporally invariant, with an optical depth determined by the variable τ. This aerosol layer is parameterized to have

a net cooling effect; and it was found that $\tau = 0.12$ might be a more reasonable choice for snowball Earth simulations than the default $\tau = 0.28$ (Liu et al. 2013). Ozone is prescribed to be at the level of the preindustrial period, which varies spatially and monthly (Rosenbloom et al. 2011). CFCs are removed. The orbital configuration is fixed to be the same as that at year 1990.

The albedo of bare sea ice depends on both sea-ice thickness and ice-surface temperature. The albedo for cold ($T_s < -1$ °C) and thick sea ice (>0.5 m) is assumed to be 0.73 in the visible band and 0.33 in the near infrared. It is assumed to decrease with decreasing thickness according to an inverse tangent relationship, and with higher temperature due to the formation of melt ponds at the surface. More details can be found in Briegleb et al. (2004). The importance of this parameterization for snowball Earth formation has been discussed in detail in Yang et al. (2012a, b). The albedo of land ice in CCSM3 is 0.8 in the visible band and 0.55 in the near-infrared band (Oleson et al. 2004). The control simulations for the bifurcation point analysis to be performed will always be initialized from a state with zero sea ice.

For these analyses, the ocean depth will be fixed at 3500 m for all experiments regardless of land-ice volume. To avoid numerical instability associated with the assumption of a flat-bottom ocean, a straight north–south oriented Gaussian ridge 2000 m in height and 70° in width is added in the Northern Hemisphere (see Figs. A1 and A2 of Liu et al. (2013)) for both continental configurations. To avoid numerical instability associated with the geographic poles, two circular polar islands of radius ~5° are added to the poles, similar to (Liu et al. 2013). The ocean circulation will be initialized from a state of rest with an initial ocean temperature that is horizontally uniform but vertically decreasing from 24 °C at the surface to 9 °C in the abyss. The initial salinity of the ocean is assumed to be uniform with a value of 35 psu.

The horizontal resolution of the atmosphere and land components is fixed to T31 (~3.75° × 3.75°), and that of the ocean and sea-ice components to "gx3" (with 100 and 116 grid points in the zonal and meridional directions, respectively). In the vertical, the atmosphere and ocean have 26 and 25 levels, respectively. The atmosphere is also initialized from a static state with vertically and zonally uniform temperatures, which varies from 15 °C at the equator to −25 °C at the poles. The time steps for the atmosphere, ocean, land, and sea-ice components are 30, 80, 30 and 60 min, respectively. Fluxes are exchanged once every hour between the atmosphere and land, and between the atmosphere and sea-ice components, and once every day between the ocean and other components. To search for the bifurcation point, we first run CCSM3 for both continental configurations for 5000 years at $pCO_2 = 2000$ ppmv after which time the climate inevitably reaches a state of statistical equilibrium (the outputs of the last 100 years are used for analysis). These serve as control runs from which the model is branched off with successively lower values of assumed pCO_2 until a hard snowball Earth forms. The bifurcation point is then constrained to a small range by further refinement of the assumed value of pCO_2, typically a few tens of parts per million by volume (ppmv).

When the ice sheet thickness is reduced to test how this model characteristic may affect the bifurcation point, the ocean and sea ice are initialized from the equilibrium state obtained for the original ice sheets while the atmosphere and land are initialized from some arbitrary state as above (this method will be referred to as involving a hybrid run in CCSM3). The model is again run to a new equilibrium state at $pCO_2 = 2000$ ppmv, which typically requires an additional integration of approximately 1500 model years. The bifurcation point is then re-determined.

2.4 CAM3 configuration

The results from the CCSM3 to be discussed in Sect. 3 demonstrate that the climate becomes significantly colder when the thickness of the continental ice sheets is reduced. In order to identify the mechanism that is responsible for such cooling, we turn to CAM3 coupled with a slab ocean of 50 m depth so as to reduce the number of processes in the modeled climate. The same resolution of T31, as used in the atmosphere component of the CCSM3 model, is used for CAM3. To further simplify the problem, an idealized continental configuration is employed, which is flat and rectangular (in a cylindrical map projection), centered on the equator (Fig. 5). The surface of the continent is assumed to be covered by a flat ice sheet. The ocean heat transport, in the absence of a good argument to the contrary, is assumed to be uniformly zero. Trials with other forms of ocean heat transport, e.g., those from CCSM3 simulations, revealed that it is difficult to obtain soft snowball solutions for different ice-sheet surface elevations under the same external climate forcing (e.g., CO_2 forcing). The ozone and aerosols are set to be identical to those specified in the CCSM3 model as described above.

Four pairs of simulations are carried out, and the ice surface elevations of members 1 and 2 of each pair are fixed to 4 and 2 km, respectively. The solar insolation and pCO_2 are different for each pair of simulations (see Table 2 for their values) in order for the obtained climate states to be similar to the 100 and 50 % thickness cases obtained by CCSM3 (Fig. 8). In the first pair of experiments (DEFAULT), the CAM3 model coupled with a slab ocean is run to equilibrium; all physical processes operate as in the default settings of CAM3 and the slab ocean. This is to determine whether the result in CCSM3 that thinner ice sheets result

Table 2 Configuration of the CAM3 experiment pairs

	Continent	Sea ice	Cloud	Water vapor	Solar insolation (W m^{-2})	pCO_2 (ppmv)	Diff. in SST[a] over ocn (°C)	Heat transp. to land (W m^{-2})
DEFAULT	Equator	Yes	Yes	Yes	1325	12,800	−11.47	41.8 (39.9)[b]
NoCldNoSI	Equator	No	No	Yes	1285	1000	−2.63	82.1 (64.8)
DRY	Equator	No	No	No	1285	1500	−0.80	16.4 (7.7)
DryNoCO_2	Equator	No	No	No	1285	0	−0.49	11.7 (5.3)

In each pair, the two experiments differ only in the surface elevation; one is 4 km, the other 2 km

[a] The difference in sea surface temperature (SST) is calculated by subtracting the SST of the 2 km case by that of the 4 km case. In the dry atmosphere experiments, the SST is the surface temperature averaged over the land area not covered by ice sheets

[b] The values in the brackets are for experiments in which the ice sheet thickness = 4 km

in a colder climate can be recovered in this much simpler model, and whether feedback associated with dynamic oceanic and sea-ice processes may play significant roles in cooling the climate when the ice-sheet thickness is reduced. In the second pair of experiments (NoCldNoSI), sea ice is removed but sea surface temperature is allowed to drop below the freezing point of seawater (e.g., −1.8 °C), and the radiative effect of cloud is removed as well. In the third pair of experiments (DRY), the atmosphere is assumed to be entirely dry, i.e., all water and water vapor are removed so that there is no feedback due to the presence of water vapor and snow. In the final pair of experiments (DryNoCO_2), the atmosphere is not only dry but also free of all greenhouse gases. These experiments are summarized in Table 2. All simulations are run for 33 years except for the first pair that are run for 50 years, and the mean results from the last 3 years of the runs are compared.

3 Results and discussion

3.1 Influence of ice-sheet presence on climate

The control climate, defined as the equilibrium climate at 94 % of the present-day solar insolation and 2000 ppmv pCO_2, is obtained for each continental configurations, namely, those for 720 and the 570 Ma. Compared to the control climate obtained in Liu et al. (2013) where no ice sheet was considered, the control climate for each of our model configuration is significantly colder, as expected, and the sea-ice edge is much closer to the equator (Fig. 3). This is not surprising since the presence of the continental ice sheets increases surface albedo substantially. The differences between the two control climates obtained here and those in Liu et al. (2013) are analyzed using the simple 1-D EBM in Heinemann et al. (2009). This model quantifies the contribution of planetary albedo, emissivity and oceanic-plus-atmospheric heat transport to the zonal-mean difference in surface temperature between the two equilibrium states. The results of the 1-D EBM clearly indicate that the higher planetary albedo is the main reason why the climate is colder when ice sheets are assumed to cover the continents (Fig. 4), since the planetary albedo is largely determined by the surface albedo over land ice, sea ice or snow (not shown).

The feedbacks from sea-ice area expansion and water vapor reduction also contribute substantially to the cooling by increasing surface albedo and reducing greenhouse effect, respectively. The influence of the expansion of sea-ice area is most clearly seen in the Northern Hemisphere, where the minimum of the red curve in Fig. 4 indicates the shift of ice edges towards the equator in Fig. 3b, d relative to that in Fig. 3a, c, respectively. Only within the tropical region are the influence of the continental ice sheets on planetary albedo and thus on surface temperature easily identified, since sea ice is absent in the tropics (Fig. 3). The water–vapor content in the atmospheric column is reduced significantly in the colder climate (Fig. 5), and contributes to the cooling due to the decrease of its greenhouse effect. This can be inferred from the contribution of emissivity to the cooling (blue curves in Fig. 4). The emissivity includes the effects of both water vapor and cloud (and minor effects of other atmospheric components), where the former may be playing a major role because the radiative effect of the cloud turns out to be warming in CCSM3 (Fig. 6).

The shortwave cloud forcing and longwave cloud forcing change in opposite directions when the continents are covered by ice sheets. The former becomes less negative (a warming effect) at almost all latitudes, due to the reduction of low-level cloud fraction (not shown) and the increase of surface albedo. The latter becomes less positive (a cooling effect) due to a substantial reduction of high-level cloud fraction (not shown). The net effect of the two is one of warming. The effect of cloud (the magnitude or even the sign of its radiative forcing) is of course highly model-dependent (Cess et al. 1990), and as a consequence we will

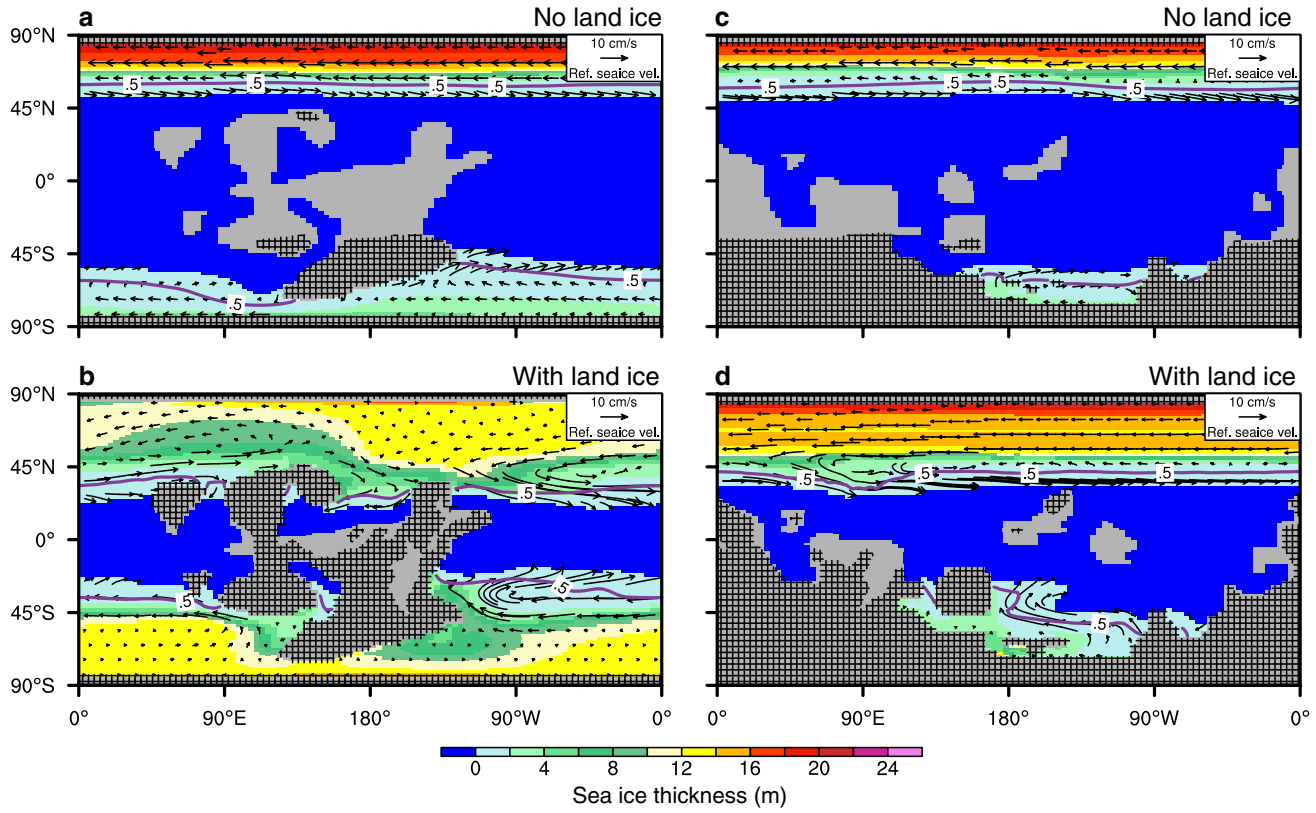

Fig. 3 Annual mean sea-ice thickness (*filled contours*) and velocity (*arrows*) of the control climates, for which the solar insolation is 94 % of the present-day value and pCO_2 is 2000 ppmv. The two *top panels* (**a**, **c**) are the climate states obtained by Liu et al. (2013) when land-ice sheets were not considered, the two *bottom panels* (**b**, **d**) are obtained in this study with the continents fully covered by ice sheets (see Fig. 1). The 720 Ma continental configure is on the *left*, and the 570 Ma on the *right*. The *dark blue area* is open ocean, and the *grey area* is continent. The hatched regions are where land-snow thickness is more than 1 cm. All sea-ice areas with grid-box fraction >1 % are plotted, and the *purple curves* for grid-box fractions of 50 % are also indicated

not stress its role in influencing the climate state when continental ice sheets are considered.

The heat transports of ocean and atmosphere act to warm the mid latitudes near the sea-ice edges (~30°N and 30°S, Fig. 3). This is consistent with previous studies, demonstrating that the wind-driven ocean circulation intensifies and transports heat to the sea-ice edges, inhibiting them from moving further towards the equator (Poulsen et al. 2001; Poulsen and Jacob 2004; Yang et al. 2012a, b). The net effect of the oceanic-plus-atmospheric heat transport is close to 0. Therefore, heat transport has very little net contribution to the globally averaged temperature difference between the climate with and without continental ice sheets. However, the ocean heat transport could have an important indirect effect, by changing the sensitivity of climate to sea-ice albedo (B. Rose, in preparation).

3.2 Hard snowball Earth bifurcation points

The bifurcation points for the 720 and 570 Ma continental configurations fully covered by land ice are determined to be between 600–630 and 300–320 ppmv, respectively (Fig. 7), when complete continental ice cover is assumed and when transient evolution of the ice sheets is neglected. In contrast, the bifurcation points for the two continental configurations were shown to be located at the much lower values of ~60 and ~100 ppmv for the two continental configurations, respectively, when the influence of land ice was neglected (Liu et al. 2013). Moreover, and as expected the equatorially located 720 Ma continental configuration enters a hard snowball state more easily than the more poleward 570 Ma continental configuration, which is now contrary to the finding of Liu et al. (2013) in which the influence of continental ice cover was neglected. Clearly, the albedo effect of a large area of low-latitude ice overwhelms all of the previously identified mechanisms that otherwise serve to cool the 570 Ma continental configuration surface more efficiently. These previous mechanisms include more negative cloud forcing and enhanced sea-ice transport near the edge of sea ice, more snow coverage on land in the mid to high-latitude region (Poulsen et al. 2002; Liu et al. 2013), and a more humid (cloudy) tropical region

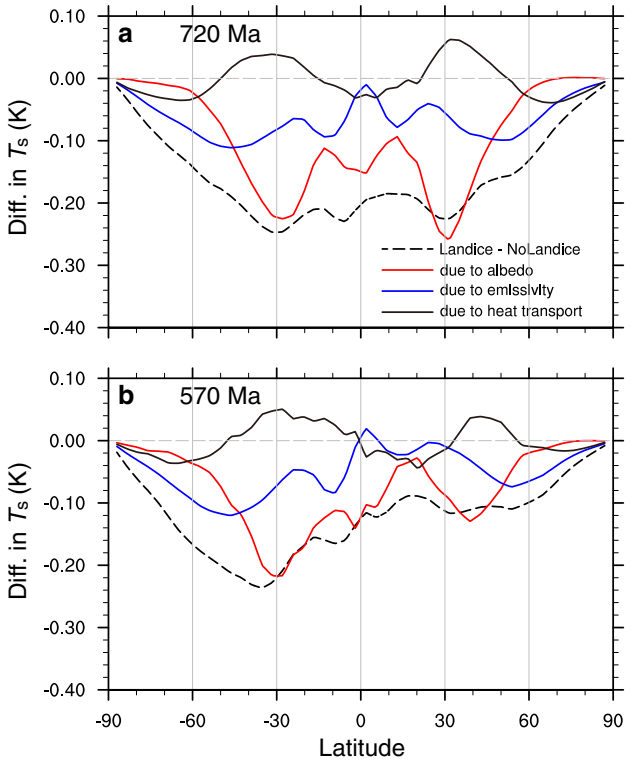

Fig. 4 Difference in zonal-mean surface temperature (*black dashed curves*) between the climate obtained with and without continental ice sheets (Fig. 1). Solar insolation is 94 % of the present-day value and pCO_2 is 2000 ppmv for *both panels*. The results are averaged over the last 100 years of the respective runs. The contributions of planetary albedo (*red curves*), emissivity (*blue curves*) and atmosphere-plus-ocean heat transport (*black curves*) to the difference in surface temperature are calculated using a 1-D EBM model (e.g., Heinemann et al. 2009). Note that all values have been weighted by the ratio of the area of the corresponding latitudinal band of 1° to the total area of the Earth. **a**, **b** For 720 and 570 Ma, respectively

(Fiorella and Poulsen 2013) in the more poleward continental configuration such as that for approximately 570 Ma.

When the thickness of continental ice sheets is reduced to 75 % of the initial value, the bifurcation point is shifted upward into the interval 700–800 ppmv for the 720 Ma continental configuration. When the thickness is thinned further to an implausible degree (see Sect. 2.2), the bifurcation point increases dramatically (Fig. 9). It is higher than 900 ppmv for 50 % ice thickness and higher than 1500 ppmv for 25 % ice thickness. We have also performed a single test for the 570 Ma continental configuration, and the result is consistent in terms of the shift of the bifurcation point with the results for the 720 Ma continental configuration (not shown). We stress that the impacts of reductions in ice sheet thickness are explored here solely as a means of assessing the uncertainties that might result from the use of different models; we do not imagine that the reductions explored are caused by warming. Thickness reduction caused by warming will cause exposure of bedrock near the edges of the ice sheets and therefore substantial reduction of the surface albedo (e.g., Liu and Peltier 2010). Here the area of the ice sheet is fixed to ensure the state of a soft snowball Earth, thus high surface albedo is retained and climate remains cold. However, we still find this result to be counter intuitive because lowering topography usually increases the surface temperature of the land (or ice sheet), based on the assumption of a fixed lapse rate, and could thereby result in a warming of the entire atmosphere. The mechanism underlying this unexpected behavior of the model is analyzed next.

3.3 Cooler climate for thinner ice sheets

The globally averaged annual-mean surface temperatures obtained for different ice sheet thicknesses at

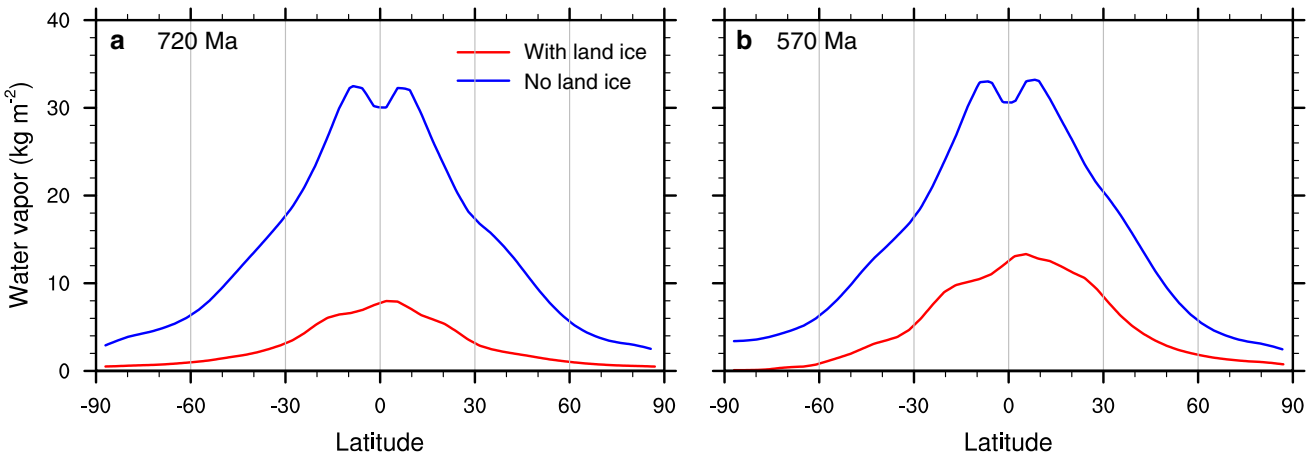

Fig. 5 Zonal-mean total water vapor in the atmospheric column when the continents are covered by ice sheets (*red*) or are ice free (*blue*). Solar insolation is 94 % of the present-day value, and pCO_2 is 2000 ppmv in all four simulations

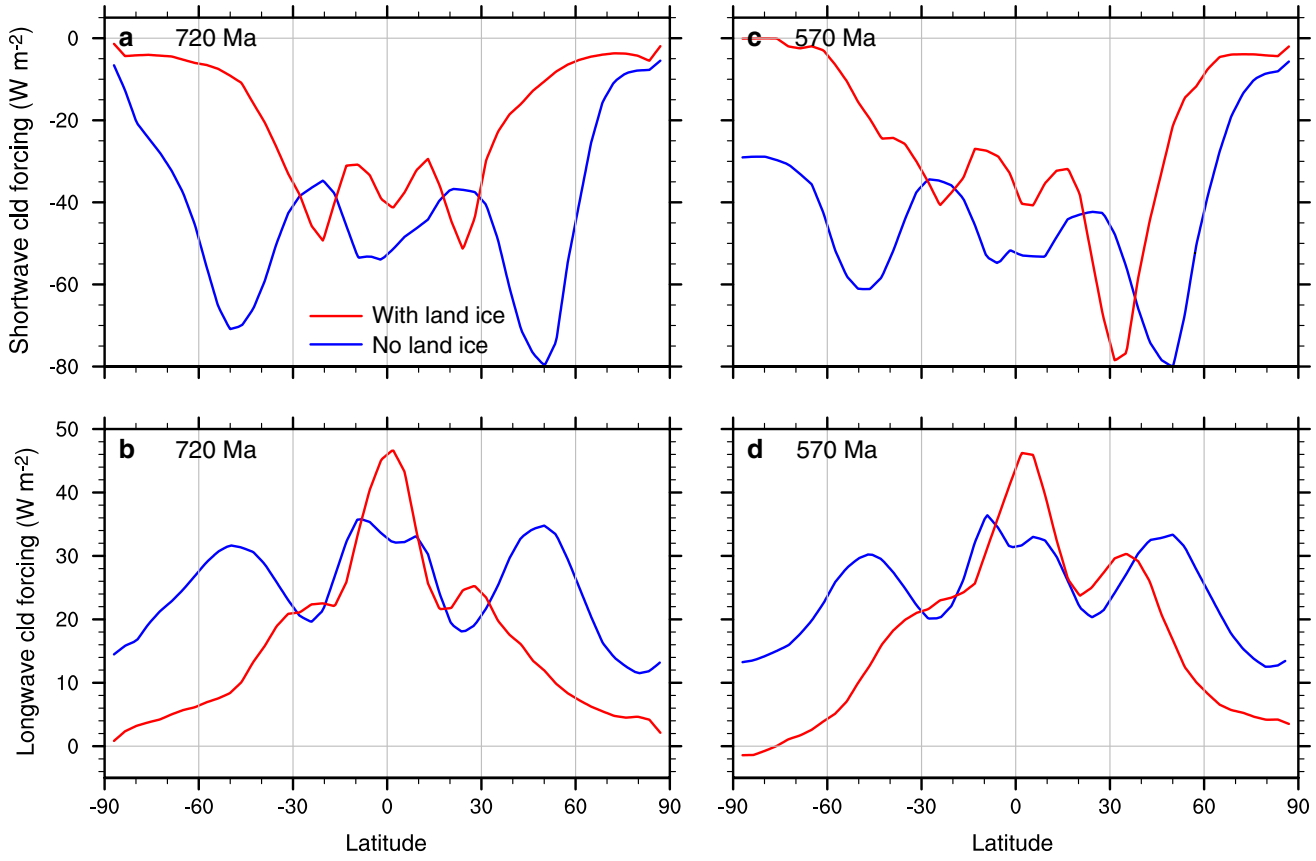

Fig. 6 Zonal-mean shortwave and longwave cloud forcing when the continents are covered by ice sheets (*red*) or are ice free (*blue*). Solar insolation is 94 % of the present-day value, and pCO_2 is 2000 ppmv in all four simulations. **a**, **b** For the 720 Ma continental configuration; **c**, **d** For 570 Ma

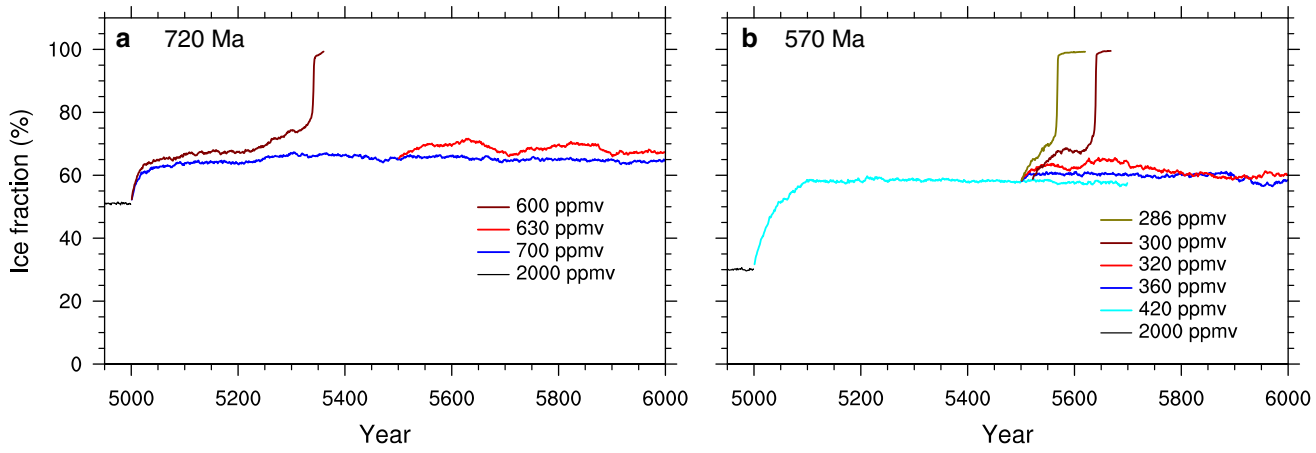

Fig. 7 Time series of global-mean sea-ice coverage. It is calculated as the total sea-ice area divided by total ocean area, and a hard snowball Earth forms when the value reaches 100 %. The short *black curve* at the beginning of the time series shows the last 50 years of the control run, from the end of which the climate model is branched off (*colored curves*) with reduced pCO_2

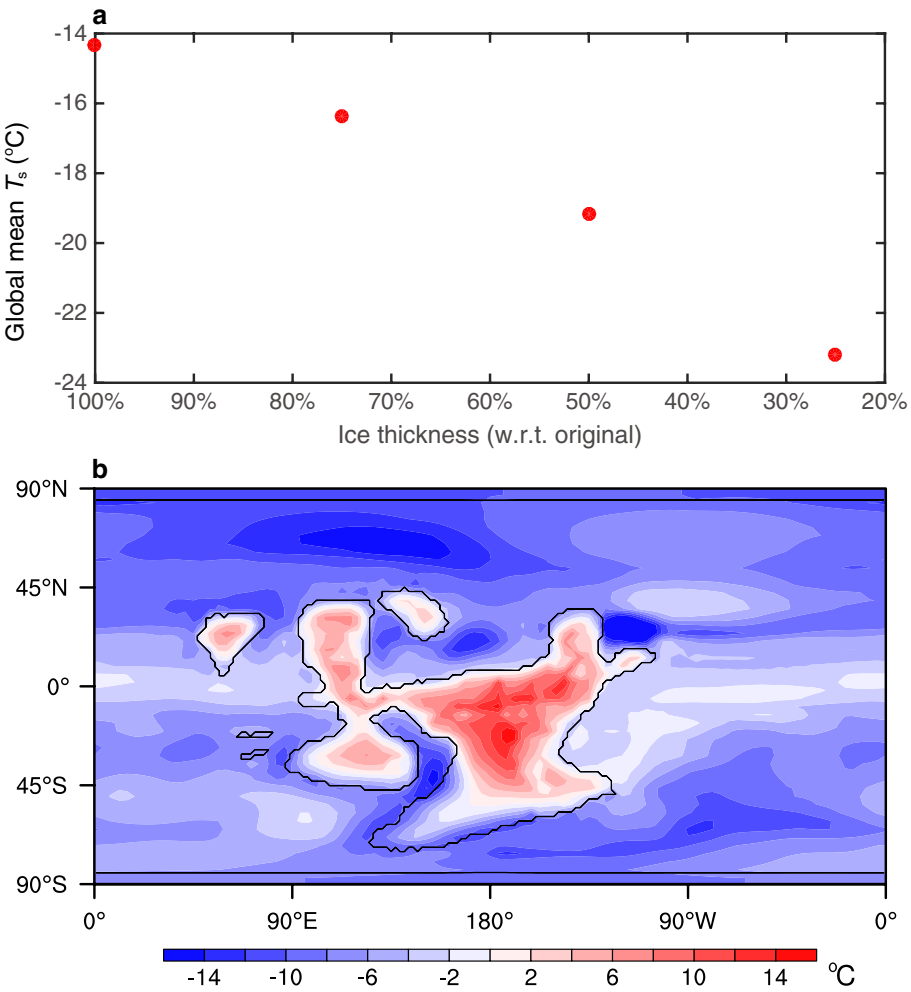

Fig. 8 **a** Globally averaged annual mean surface temperatures for different ice-sheet thicknesses, which are expressed as percentages of the thickness of the ice sheets obtained by the coupled ice-sheet model and EBM (see text for more information); **b** The pattern of the difference in surface temperature between the 50 % thickness case and the 100 % thickness case (former minus latter)

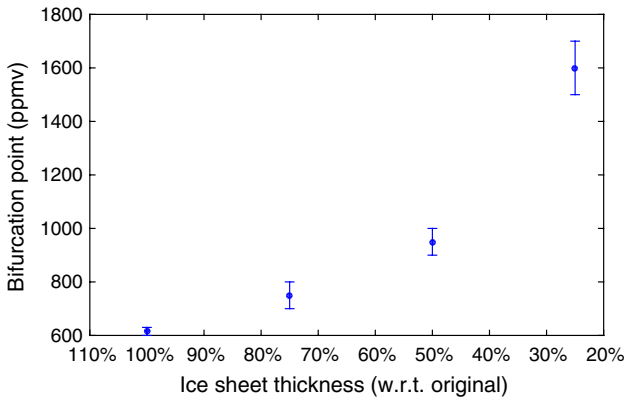

Fig. 9 The hard snowball bifurcation points obtained using CCSM3 for the 720 Ma continental configuration for different ice-sheet thicknesses, which are expressed as percentages of the thickness of the ice sheets obtained using the coupled ice-sheet model and EBM (see text for more information). The *error bars* only indicate the precision in determining each snowball bifurcation point, which could be reduced by carrying out further simulations (see text for how the bifurcation points are determined)

$pCO_2 = 2000$ ppmv are shown in Fig. 8a. The temperature decreases monotonically when the ice-sheet thickness, and thus its topographic height is reduced. Taking the 50 and 100 % ice thickness runs as examples, the spatial distributions of the difference (the former minus the latter) in annual-mean surface temperature is shown in Fig. 8b. The temperature over the ice sheets increases due to the lowering of surface elevation as expected; the more the elevation is reduced the higher the temperature rises, which is indicated by the larger temperature increase in the interior of the ice sheets where the elevation changes more significantly. The oceans, however, become cooler when the ice sheets are thinned which is the reason why the bifurcation points shift to higher values. Figure 9 plots the shift of the bifurcation point determined using the CCSM3 integrations as a function of the extent to which the ice sheets are thinned relative to the control case. The thinner the ice sheets or the lower their surface height relative to the sea level, the higher the value of pCO_2 at which bifurcation into the hard snowball state would occur. An important

implication may be that, if the control model ice sheets were emplaced on initially high topography with respect to sea level then the *p*CO2 required to induce transition into the hard snowball state would be lower than approximately 600 ppmv for our model of the Sturtian configuration.

We resort to the use of the atmosphere-only model CAM3 to identify the process that is responsible for the cooling of the oceans, which accompanies the increase of the pCO_2 bifurcation point with decreasing ice-sheet thickness or equivalently decreasing ice-sheet surface height relative to the sea level. This key process, through gradual simplifications of the model, as will be described in detail in what follows, is found to be due to the enhancement of atmospheric heat transport from the ocean-covered regions to the ice sheet-covered regions when the ice sheets are thinned.

The results for the experiments DEFAULT, which use the atmosphere-only CAM3 model, are consistent with that of the fully coupled CCSM3 structure; when ice-sheet surface elevation is reduced from 4 to 2 km, the surface temperature increases over the ice sheet but decreases significantly over the ocean (Fig. 10a). The magnitudes of surface temperature decrease (~14 °C) over the ocean are similar between CAM3 and CCSM3 (compare Figs. 8b, 10a). This implies that dynamical processes of both ocean and sea ice do not play a key role in the cooling of the ocean.

When the sea ice and the radiative effect of cloud are removed (experiments NoCldNoSI), the cooling of the ocean due to the thinning of the ice sheets is still significant (Fig. 10b). The effect of removing only sea ice is also analyzed, and the result is quite similar to that in Fig. 10b (not shown). The cooling in the experiments NoCldNoSI is much smaller than that in the experiments DEFAULT, indicating that the sea-ice albedo feedback is very important in enhancing the cooling. However, the presence of overall cooling of the ocean in the experiments NoCldNoSI suggests that neither the sea ice nor the influence of cloud triggers the cooling when the ice-sheet surface elevation is lowered.

The results of experiments DRY, in which (implicitly) no ocean exists and no water vapor is present (thus no cloud, snow and latent heat flux) in the atmosphere, are still broadly consistent with those of CCSM3 (Fig. 10c). However, it is now evident that the cooling of the ocean is much less uniform spatially, particularly in parts of the polar regions, and warming occurs when the ice sheets are thinned. This further demonstrates the importance of the water–vapor feedback, which has the effect of cooling the ocean more significantly and uniformly in the previous experiments in this sequence based on the simplified CAM3 model. Note that the surface temperature increase over the ice sheets when the elevation of the ice sheets

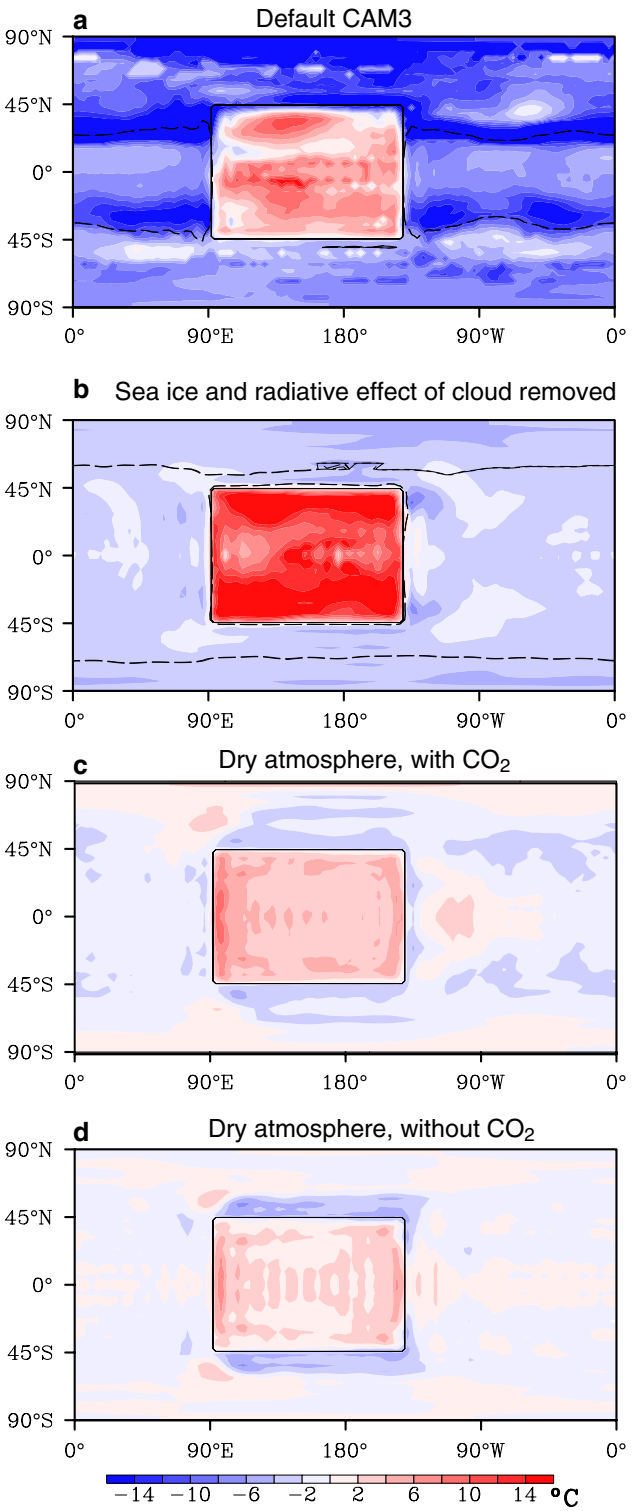

Fig. 10 Changes of surface temperature in experiments. **a** DEFAULT, **b** NoCldNoSI, **c** DRY, and **d** DryNoCO$_2$ when ice thickness is reduced from 4 to 2 km. The boundary of the continent/ice sheet is indicated by the *solid black curve*. The sea-ice boundary in (**a**) and the −1.8 °C contour in (**b**) for the 4 km case are indicated by *black dashed curves*

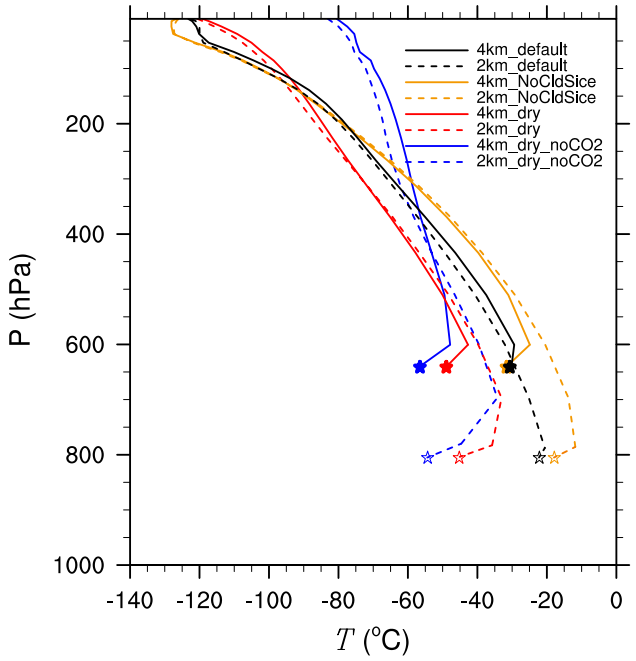

Fig. 11 Vertical profiles of temperature averaged over the ice sheet-covered region, for experiments DEFAULT, NoCldNoSI, DRY and DryNoCO$_2$. The corresponding radiative surface temperature for each profile is indicated with a star (*filled star* for *solid curve* and *open star* for *dashed curve*)

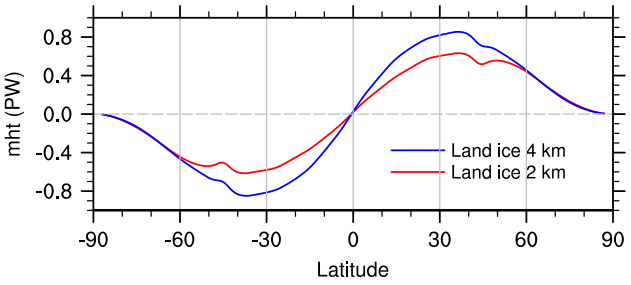

Fig. 12 Meridional heat transport of the atmosphere in experiments DRY, in which neither water nor water vapor is present in the system

is reduced from 4 to 2 km is much smaller than those in experiments DEFAULT and NoCldNoSI. This gives rise to the illusion that the lapse rate in a dry atmosphere must be much smaller than that in the moist atmosphere. The cause of this illusory inference is that, in the dry atmosphere, there is a highly significant temperature inversion developed near the surface of the ice sheets (see the red and blue curves in Fig. 11), similar to that in the polar regions (especially in winter) of the modern Earth (e.g., Kahl 1990; Ackerman et al. 1998) and that in the winter hemisphere of a hard snowball Earth (Pierrehumbert 2005). At elevations above the temperature inversion, the lapse rate over the ice sheets in the dry atmosphere is in fact large.

Another process that needs to be considered for the cooling of the ocean regions is the shifting of air mass from over the ocean to over the ice sheets when the ice sheets are thinned. The air mass, and thus the pressure of the air over ocean decreases if the total air mass is conserved as it is in both CCSM3 and CAM3. This weakens the greenhouse effect of CO_2 due to the reduced pressure broadening of the absorption spectra of this gas, therefore may cause cooling over the oceans. The surface pressure over the oceans is diagnosed to decrease only slightly, <5 % for the realistic continental configurations and ice sheets even when the ice sheets are thinned by 50 %. A simple calculation with a single column model CliMT (a Python climate modelling and diagnostic toolkit available at http://github.com/rodrigo-caballero/CliMT), which is configured to use the same radiative module as CAM3 indicates that the radiative forcing is not only small (<1 W m^{-2}) but also opposite in sign to what would be required to explain the observation. The reason for this is that although the weakening of the pressure broadening effect on CO_2 has a slight cooling effect in the longwave band, the reduced mass of the N_2 and O_2 scatters less sunlight and has a warming effect in the shortwave band that is larger (see also Poulsen et al. 2015), the net effect being one of warming. The calculation based on CAM3 in experiments DryNoCO$_2$ confirms this, showing that in an atmosphere without greenhouse gases, the cooling over the ocean still occurs (Fig. 10d).

Therefore, none of processes in the climate system tested through the preceding analyses has been shown to be primarily responsible for the cooling over the ocean when ice sheets are thinned; the only remaining process is that associated with the dry dynamics of the atmosphere itself. The circulation of the atmosphere is clearly such that it transports energy from the region over the relatively warm ocean to the much colder ice sheet covered continent, in addition to its more general characteristic, which is to transport energy from the low-latitudes to the mid- to high-latitude region. This is most clearly seen from the dry atmosphere experiments DRY, which shows that the atmospheric heat transport to the mid-latitude region is much reduced when the ice sheets are thinned (Fig. 12).

The net energy input to the air mass over the ice-sheet-covered continent by sensible heat transport can be simply calculated using the radiative imbalance at the top of the atmosphere over the same region, since at equilibrium the net energy flux into the air mass should be 0. This calculation demonstrates that the dry atmospheric heat transport convergence (experiments DryNoCO$_2$), averaged over the area of the ice sheet covered continent, increases from 5.3 to 11.7 W m^{-2} when the ice sheets are thinned from 4 km to 2 km. For the wet atmosphere, e.g., in experiments NoCldNoSI, this value increases from 64.8 to 82.1 W m^{-2}. These values correspond to a direct negative forcing of

~1.7 and 4.3 W m^{-2} over the ocean, respectively. Values for other experiments are listed in Table 2.

For the CCSM3 simulations with more realistic continents and ice sheets corresponding to 720 Ma, this negative forcing over the ocean is only ~0.5 W m^{-2} when the ice sheets are thinned uniformly by 50 %. This value is very similar to that of the CAM3 experiments DEFAULT. This seems to be contradictory to the large cooling obtained in these experiments. The exact mechanism is unclear, but the sea-ice feedback is clearly playing an important role. We speculate that as the sea ice grows, the cooling of the planet, especially the ocean, is then sustained mainly by the high surface albedo, not by the enhanced atmospheric heat transport that removes energy from the ocean area. The growth of sea ice therefore weakens the atmospheric heat transport towards the ice sheet covered area. However, we have yet to understand the process of dynamic adjustment that is responsible for this weakening. Indeed, at the beginning of the simulations when the ice sheets are just thinned, the energy deficit at the top of atmosphere over the ice-covered supercontinent is large, approximately 30 and 15 W m^2 for the CCSM3 and the CAM3 experiments DEFAULT, respectively, but both gradually decrease to about 2 W m^{-2} once the climate system reaches an equilibrium. This decrease of energy deficit is observed for other experiments too, but the magnitude of the decrease is much less dramatic.

It is relatively straightforward to understand why energy input to regions covered by land ice must increase when the ice sheets are thinned. Dynamically, since the thickness of the air over the ice sheets increases, this enables larger exchange of mass and energy with the surrounding warm regions over the oceans. The influence of this energy sink does not reach very far into the ocean area if the atmosphere is dry (Fig. 10c), but gives the illusion that it reaches the whole globe due to the feedback of water vapor (Fig. 10b).

4 Conclusions

We have determined the hard snowball CO_2 threshold (or bifurcation point) for both the 720 and 570 Ma continental configurations using CCSM3 under the assumption that the solar insolation for both periods may be approximated by a 6 % reduction relative to the modern level. Different from those previously performed experiments, the supercontinents in this study were assumed to be fully covered by prescribed ice sheets, i.e. a soft snowball Earth was assumed to be the initial condition. In terms of ice-sheet area, the bifurcation points obtained in this way provide upper bounds on the critical pCO_2; these bifurcation points would be lower if the area of continental ice sheets were smaller.

The influence of the uncertainty in the thickness of ice sheets on the bifurcation points was investigated. We demonstrated that when the ice sheets are thinner, the climate can be significantly cooler and the bifurcation point is shifted to a higher value of pCO_2. This cooling was shown to be caused by increased atmospheric heat transport into the ice-covered continental regions, which extracted energy from the surrounding ocean regions, leading to their cooling. The associated sea ice and water vapor feedbacks enhance this cooling substantially. The dynamics of ocean and sea ice and the feedback of cloud play insignificant roles in the cooling.

Therefore, in terms of ice-sheet thickness, the bifurcation points determined herein provide lower bounds on the critical pCO_2 because the ice sheets estimated with an ice-sheet model coupled to an EBM are probably the thickest. For these thickest ice sheets, the bifurcation points are between 600–630 and 300–320 ppmv for the 720 and 570 Ma continental configurations, respectively. These are 10 times and 3 times higher than their respective values when the continental ice sheets are ignored (Liu et al. 2013). This is mainly due to high surface albedo of the ice sheets, but the feedbacks from sea-ice area expansion and water–vapor reduction are important as well. The feedback of cloud in the model we employed is negative, i.e. this feedback inhibits the climate cooling.

If the ice sheets from a more advanced, ice-sheet model coupled with an AOGCM were found to be thinner than we have assumed than bifurcation point will be higher. Taking the 720 Ma continental configuration as an example, if the ice sheets are thinner than assumed above by 25 %, the bifurcation point shifts to between 700 and 800 ppmv. We argue that the ice sheets are unlikely to be much thinner than this for the reasons given in Sect. 2.2. Therefore, we conclude that the hard snowball Earth bifurcation points are expected to be close to 700 and 350 ppmv, with possible ranges of 600–800 and 300–400 ppmv, for the 720 and 570 Ma continental configurations, respectively. These are much higher values than previously obtained with the same model but without including the continental ice sheets. These results suggest that formation of a soft snowball Earth for equatorially distributed continents may be more challenging than previously thought, as it would have to form at pCO_2 higher than ~600 ppmv. The present study, however, does not rule out such possibility as it has not considered the development and dynamics of continental ice sheets. On the other hand, an implication that we have not explicitly discussed in detail is that if low-latitude continental ice sheets were emplaced on a supercontinent with high topographic relief, the bifurcation point for transition into a hard snowball state would be shifted to lower values of pCO_2 according to the trend in Fig. 9, how much lower would depend upon the nature of the topography of

the supercontinent. In other words, ice sheets that extend to higher elevation warm the ocean surface and hereby inhibit the transition to a hard snowball Earth.

All of the analyses reported herein, aside from being based upon the neglect of transient ice sheet evolution, have also been based upon the neglect of plausible ocean carbon cycle feedbacks that could well, by themselves, prevent atmospheric pCO_2 from decreasing to the level required to cause transition into a hard snowball state (Peltier et al. 2007; Liu and Peltier 2011). We view the current paper as contributing, nevertheless, to efforts to more accurately bound the conditions under which Neoproterozoic glaciations might have developed and the nature of the sea-ice cover over the oceans that would have accompanied them. These bounds remain rather loose at present, although modern coupled atmosphere–ocean–sea ice models are contributing to their refinement. The assumption that a soft snowball Earth forms before entering a hard snowball Earth is critical to the analyses conducted in this study, yet it has proven possible so far with only models of intermediate complexity (e.g., Liu and Peltier 2010). Whether a soft snowball Earth can form is clearly critical to the understanding of Neoproterozoic glaciations. The present work constitutes the necessary first step towards the more demanding analyses upon which we will focus next, in which the transient evolution of a GCM coupled ice sheet model will be employed to further refine our understanding of the hard snowball bifurcation points.

Acknowledgments We thank Z.X. Li at Curtin University of Australia and W.T. Hyde for providing the continental boundary conditions that were used to construct the 720 and 570 Ma land–ocean masks, respectively. We are grateful to the three anonymous reviewers whose suggestions have improved both the presentation and the science content of the paper. The CCSM3 simulations were performed on the SciNet facility at the University of Toronto, which is a component of the Compute Canada HPC platform, while the CAM3 simulations were performed on the supercomputer at the LaCOAS facility of Peking University. Y. Liu is supported by the Startup Fund of the Ministry of Education of China. The research of WRP at the University of Toronto is supported by NSERC Discovery Grant A9627.

References

Ackerman SA, Strabala KI, Menzel WP, Frey RA, Moeller CC, Gumley LE (1998) Discriminating clear sky from clouds with MODIS. J Geophys Res Atmos 103(D24):32141–32157. doi:10.1029/1998jd200032

Bahcall JN, Pinsonneault MH, Basu S (2001) Solar models: current epoch and time dependences, neutrinos, and helioseismological properties. Astrophys J 555(2):990–1012. doi:10.1086/321493

Bodiselitsch B, Koeberl C, Master S, Reimold WU (2005) Estimating duration and intensity of Neoproterozoic snowball glaciations from Ir anomalies. Science 308(5719):239–242. doi:10.1126/science.1104657

Briegleb BP, Bitz CM, Hunke EC, Lipscomb WH, Holland MM, Schramm JL, Moritz RE (2004) Scientific description of the sea ice component in the Community Climate System Model, version three. NCAR technical note NCAR/TN-463 + STR:78. doi:10.5065/D6HH6H1P

Cess RD, Potter GL, Blanchet JP, Boer GJ, Delgenio AD, Deque M, Dymnikov V, Galin V, Gates WL, Ghan SJ, Kiehl JT, Lacis AA, Letreut H, Li ZX, Liang XZ, Mcavaney BJ, Meleshko VP, Mitchell JFB, Morcrette JJ, Randall DA, Rikus L, Roeckner E, Royer JF, Schlese U, Sheinin DA, Slingo A, Sokolov AP, Taylor KE, Washington WM, Wetherald RT, Yagai I, Zhang MH (1990) Intercomparison and interpretation of climate feedback processes in 19 atmospheric general-circulation models. J Geophys Res Atmos 95(D10):16601–16615. doi:10.1029/Jd095id10p16601

Chandler MA, Sohl LE (2000) Climate forcings and the initiation of low-latitude ice sheets during the Neoproterozoic Varanger glacial interval. J Geophys Res Atmos 105(D16):20737–20756. doi:10.1029/2000jd900221

Collins WD, Bitz CM, Blackmon ML, Bonan GB, Bretherton CS, Carton JA, Chang P, Doney SC, Hack JJ, Henderson TB, Kiehl JT, Large WG, McKenna DS, Santer BD, Smith RD (2006) The community climate system model version 3 (CCSM3). J Clim 19(11):2122–2143. doi:10.1175/Jcli3761.1

Crowley TJ, Hyde WT, Peltier WR (2001) CO_2 levels required for deglaciation of a "near-snowball" Earth. Geophys Res Lett 28(2):283–286. doi:10.1029/2000gl011836

Dalziel IWD (1997) Neoproterozoic–Paleozoic geography and tectonics: review, hypothesis, environmental speculation. Geol Soc Am Bull 109(1):16–42

Donnadieu Y, Fluteau F, Ramstein G, Ritz C, Besse J (2003) Is there a conflict between the Neoproterozoic glacial deposits and the snowball Earth interpretation: an improved understanding with numerical modeling. Earth Planet Sci Lett 208(1–2):101–112. doi:10.1016/S0012-821x(02)01152-4

Donnadieu Y, Ramstein G, Fluteau F, Roche D, Ganopolski A (2004) The impact of atmospheric and oceanic heat transports on the sea-ice-albedo instability during the Neoproterozoic. Clim Dyn 22(2–3):293–306. doi:10.1007/S00382-003-0378-5

Feulner G, Kienert H (2014) Climate simulations of Neoproterozoic snowball Earth events: similar critical carbon dioxide levels for the Sturtian and Marinoan glaciations. Earth Planet Sci Lett 404:200–205. doi:10.1016/J.Epsl.2014.08.001

Fiorella RP, Poulsen CJ (2013) Dehumidification over tropical continents reduces climate sensitivity and inhibits snowball Earth initiation. J Clim 26(23):9677–9695. doi:10.1175/Jcli-D-12-00820.1

Gough DO (1981) Solar interior structure and luminosity variations. Sol Phys 74(1):21–34. doi:10.1007/Bf00151270

Heinemann M, Jungclaus JH, Marotzke J (2009) Warm Paleocene/Eocene climate as simulated in ECHAM5/MPI-OM. Clim Past 5(4):785–802

Hoffman PF, Li ZX (2009) A palaeogeographic context for Neoproterozoic glaciation. Palaeogeogr Palaeoclimatol 277(3–4):158–172. doi:10.1016/J.Palaeo.2009.03.013

Hoffman PF, Schrag DP (2000) Snowball earth. Sci Am 282(1):68–75

Hoffman PF, Schrag DP (2002) The snowball Earth hypothesis: testing the limits of global change. Terra Nova 14(3):129–155

Hoffman PF, Kaufman AJ, Halverson GP, Schrag DP (1998) A Neoproterozoic snowball earth. Science 281(5381):1342–1346

Hoffman PF, Halverson GP, Domack EW, Husson JM, Higgins JA, Schrag DP (2007) Are basal Ediacaran (635 Ma) post-glacial "cap dolostones" diachronous? Earth Planet Sci Lett 258(1–2):114–131. doi:10.1016/J.Epsl.2007.03.032

Hyde WT, Crowley TJ, Baum SK, Peltier WR (2000) Neoproterozoic 'snowball Earth' simulations with a coupled climate/ice-sheet model. Nature 405(6785):425–429

Jenkins GS, Smith SR (1999) GCM simulations of snowball Earth conditions during the late Proterozoic. Geophys Res Lett 26(15):2263–2266. doi:10.1029/1999gl900538

Kahl JD (1990) Characteristics of the low-level temperature inversion along the Alaskan Arctic coast. Int J Climatol 10(5):537–548. doi:10.1002/Joc.3370100509

Lewis JP, Weaver AJ, Eby M (2007) Snowball versus slushball Earth: dynamic versus nondynamic sea ice? J Geophys Res Oceans. doi:10.1029/2006jc004037

Li ZX, Bogdanova SV, Collins AS, Davidson A, De Waele B, Ernst RE, Fitzsimons ICW, Fuck RA, Gladkochub DP, Jacobs J, Karlstrom KE, Lu S, Natapov LM, Pease V, Pisarevsky SA, Thrane K, Vernikovsky V (2008) Assembly, configuration, and break-up history of Rodinia: a synthesis. Precambrian Res 160(1–2):179–210. doi:10.1016/J.Precamres.2007.04.021

Liu Y, Peltier WR (2010) A carbon cycle coupled climate model of Neoproterozoic glaciation: influence of continental configuration on the formation of a "soft snowball". J Geophys Res Atmos. doi:10.1029/2009jd013082

Liu Y, Peltier WR (2011) A carbon cycle coupled climate model of Neoproterozoic glaciation: explicit carbon cycle with stochastic perturbations. J Geophys Res Atmos. doi:10.1029/2010jd015128

Liu Y, Peltier WR (2013a) Sea level variations during snowball Earth formation and evolution: 2. The influence of Earth's rotation. J Geophys Res Solid Earth 118:1–21. doi:10.1002/jgrb.50294

Liu Y, Peltier WR (2013b) Sea level variations during snowball Earth formation: 1. A preliminary analysis. J Geophys Res 118:1–15. doi:10.1002/jgrb.50293

Liu Y, Peltier WR, Yang J, Vettoretti G (2013) The initiation of Neoproterozoic "snowball" climates in CCSM3: the influence of paleocontinental configuration. Clim Past 9:2555–2577. doi:10.5194/cp-9-2555-2013

Macdonald FA, Schmitz MD, Crowley JL, Roots CF, Jones DS, Maloof AC, Strauss JV, Cohen PA, Johnston DT, Schrag DP (2010) Calibrating the Cryogenian. Science 327:1241–1243. doi:10.1126/science.1183325

Oleson KW, Dai Y, Bonan G, Bosilovich M, Dickinson RE, Dirmeyer P, Hoffman F, Houser P, Levis S, Niu G-Y, Thornton P, Vertenstein M, Yang Z-L, Zeng X (2004) Technical description of the Community Land Model (CLM). NCAR Technical Note NCAR/TN-495 + STR:174. doi:10.5065/D6N877R0

Peltier WR, Liu YG, Crowley JW (2007) Snowball Earth prevention by dissolved organic carbon remineralization. Nature 450(7171):813–818. doi:10.1038/Nature06354

Pierrehumbert RT (2005) Climate dynamics of a hard snowball Earth. J Geophys Res Atmos. doi:10.1029/2004jd005162

Poulsen CJ, Jacob RL (2004) Factors that inhibit snowball Earth simulation. Paleoceanography. doi:10.1029/2004pa001056

Poulsen CJ, Pierrehumbert RT, Jacob RL (2001) Impact of ocean dynamics on the simulation of the Neoproterozoic "snowball Earth". Geophys Res Lett 28(8):1575–1578. doi:10.1029/2000gl012058

Poulsen CJ, Jacob RL, Pierrehumbert RT, Huynh TT (2002) Testing paleogeographic controls on a Neoproterozoic snowball Earth. Geophys Res Lett. doi:10.1029/2001gl014352

Poulsen CJ, Tabor C, White JD (2015) Long-term climate forcing by atmospheric oxygen concentrations. Science 348(6240):1238–1241. doi:10.1126/science.1260670

Rodehacke CB, Voigt A, Ziemen F, Abbot DS (2013) An open ocean region in Neoproterozoic glaciations would have to be narrow to allow equatorial ice sheets. Geophys Res Lett 40(20):5503–5507. doi:10.1002/2013gl057582

Rosenbloom N, Shields CA, Brady E, Yeager S, Levis S (2011) Using CCSM3 for paleoclimate applications. NCAR Technical note NCAR/TN-483 + STR:81. doi:10.5065/D69S1P09

Shackleton NJ, Berger A, Peltier WR (1990) An alternative astronomical calibration of the lower pleistocene timescale based on ODP site 677. Trans R Soc Edinb Earth 81:251–261

Tarasov L, Peltier WR (1999) Impact of thermomechanical ice sheet coupling on a model of the 100 kyr ice age cycle. J Geophys Res Atmos 104(D8):9517–9545

Voigt A, Abbot DS (2012) Sea-ice dynamics strongly promote snowball Earth initiation and destabilize tropical sea-ice margins. Clim Past 8(6):2079–2092. doi:10.5194/Cp-8-2079-2012

Voigt A, Marotzke J (2010) The transition from the present-day climate to a modern Snowball Earth. Clim Dy 35(5):887–905. doi:10.1007/S00382-009-0633-5

Voigt A, Abbot DS, Pierrehumbert RT, Marotzke J (2011) Initiation of a Marinoan snowball Earth in a state-of-the-art atmosphere-ocean general circulation model. Clim Past 7(1):249–263. doi:10.5194/Cp-7-249-2011

Yang J, Peltier WR, Hu YY (2012a) The initiation of modern "soft snowball" and "hard snowball" climates in CCSM3. Part I: the influences of solar luminosity, CO_2 concentration, and the sea ice/snow albedo parameterization. J Clim 25(8):2711–2736. doi:10.1175/Jcli-D-11-00189.1

Yang J, Peltier WR, Hu YY (2012b) The initiation of modern "soft snowball" and "hard snowball" climates in CCSM3. Part II: climate dynamic feedbacks. J Clim 25(8):2737–2754. doi:10.1175/Jcli-D-11-00190.1

Yang J, Peltier WR, Hu YY (2012c) The initiation of modern soft and hard Snowball Earth climates in CCSM4. Clim Past 8(3):907–918. doi:10.5194/Cp-8-907-2012